ELSEVIER

Earth and Planetary Science Letters 197 (2002) 261–272

EPSL

www.elsevier.com/locate/epsl

Seismic evidence for a tilted mantle plume and north–south mantle flow beneath Iceland

Yang Shen [a,*], Sean C. Solomon [b], Ingi Th. Bjarnason [c], Guust Nolet [d], W. Jason Morgan [d], Richard M. Allen [d,1], Kristin Vogfjörd [e], Steinun Jakobsdóttir [f], Ragnar Stefánsson [f], B.R. Julian [g], G.R. Foulger [h]

[a] *Graduate School of Oceanography, University of Rhode Island, South Ferry Road, Narragansett, RI 02882, USA*
[b] *Department of Terrestrial Magnetism, Carnegie Institution of Washington, 5241 Broad Branch Road N.W., Washington, DC 20015, USA*
[c] *Science Institute, University of Iceland, Reykjavik, Iceland*
[d] *Department of Geosciences, Guyot Hall, Princeton University, Princeton, NJ 08544, USA*
[e] *National Energy Authority, Grensasvegi 9, Reykjavik, Iceland*
[f] *Meteorological Office of Iceland, Bustadavegi 9, Reykjavik, Iceland*
[g] *US Geological Survey, 345 Middlefield Road, Menlo Park, CA 94025, USA*
[h] *Department of Geological Sciences, University of Durham, Durham DH1 3LE, UK*

Received 7 August 2001; received in revised form 23 January 2002; accepted 25 January 2002

Abstract

Shear waves converted from compressional waves at mantle discontinuities near 410- and 660-km depth recorded by two broadband seismic experiments in Iceland reveal that the center of an area of anomalously thin mantle transition zone lies at least 100 km south of the upper-mantle low-velocity anomaly imaged tomographically beneath the hotspot. This offset is evidence for a tilted plume conduit in the upper mantle, the result of either northward flow of the Icelandic asthenosphere or southward flow of the upper part of the lower mantle in a no-net-rotation reference frame.

Keywords: mantle plumes; transition zones; discontinuities; convection; Iceland

1. Introduction

Linear chains of volcanic centers displaying regular age progressions are thought to result from zones of upper-mantle melt production that are nearly stationary with respect to the overlying tectonic plates [1]. Morgan [2] proposed that such stationary regions of melt production, or hotspots, are maintained by long-lived upwelling of warm material from the lower mantle through narrow conduits that he termed plumes. The hy-

* Corresponding author. Tel.: +1-401-874-6848; Fax: +1-401-874-6811.
E-mail address: yshen@gso.uri.edu (Y. Shen).

[1] Present address: Department of Geology and Geophysics, University of Wisconsin, 1215 W. Dayton St., Madison, WI 53706, USA.

0012-821X/02/$ – see front matter
PII: S0012-821X(02)00494-6

pothesis of fixed hotspots has provided a useful means of determining lithospheric plate motions from the geographic orientations and age distributions of volcanic chains, but the validity of this hypothesis on a global scale remains controversial [3,4]. Observational evidence for or against fixed hotspots has been derived, to date, mostly from hotspot manifestations at the Earth's surface.

The concept of fixed hotspots implies vertical plume conduits, because deflection of plume conduits by the convecting mantle – as suggested by mantle fluid dynamic models [5] – should lead to relative motions among hotspots over time scales of plate (and thus mantle-flow) reconstructions. Low-seismic-velocity anomalies in the lower mantle beneath hotspots (e.g. Iceland and Hawaii) in some global tomographic models [6,7], anomalies that usually differ in shape from vertical columns, have been suggested as evidence for tilted plumes in the lower mantle [7]. However, the ability of global models to resolve narrow, low-velocity structures in the lower mantle remains a topic of debate [8], and alternative global tomographic models fail to show a low-velocity anomaly beneath Iceland in the lower mantle [9,10].

An alternative approach to address the tilting of plume conduits in the upper mantle is to compare measures of plume influence in the shallow upper mantle with the depths to seismic discontinuities near 410- and 660-km depth, global features that have been identified with the temperature-dependent transitions of $(Mg,Fe)_2SiO_4$ from α-olivine to β-spinel (wadsleyite) and from γ-spinel (ringwoodite) to $(Mg,Fe)SiO_3$-perovskite plus (Mg,Fe)O-magnesiowüstite, respectively [11,12]. In an earlier study of mantle discontinuities beneath Iceland [13], we used receiver functions derived from body-wave records of teleseismic earthquakes from the broadband ICEMELT seismic network [14] and the permanent Global Seismographic Network station BORG (Fig. 1) to demonstrate that the transition zone is thinner than the average Earth [15] beneath central and southern Iceland but is of normal thickness beneath surrounding areas. This result is consistent with a hot and narrow plume originating from the lower mantle [13].

Additional broadband seismic data were collected during the Iceland Hotspot Project (or the HOTSPOT experiment) [16] from the spring of 1996 to the fall of 1998 (Fig. 1). The combined ICEMELT and HOTSPOT data set is approximately four times as large as the ICEMELT data used in the previous study [13]. By incorporating a substantially greater number of receiver functions than in the previous study, we are now able to identify features of the transition-zone anomaly that were not resolved earlier.

2. Data processing and signal quality

The calculation and stacking of receiver functions follow procedures described previously [13,17]. To ensure that random noise is far below the signal (the conversion of a P-wave to an S-

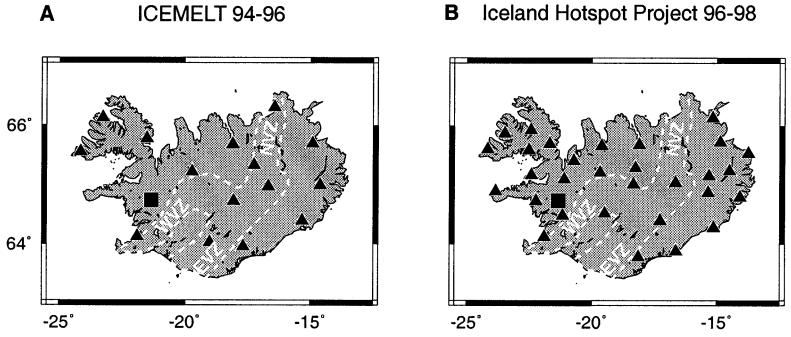

Fig. 1. Seismic stations used in the ICEMELT experiment (A) and the Iceland Hotspot Project (B). The square denotes the Global Seismic Network station BORG. Dashed lines delineate the northern (NVZ), eastern (EVZ), and western (WVZ) volcanic zones.

wave at depth d, or Pds), we select seismograms with noise levels (defined as the standard deviation of the values on the radial component in an 80-s window before the P arrival) less than 0.1 times the amplitude of the direct P-wave on the vertical component. Because many seismograms have signal-to-noise (S/N) ratios greater than 10 and because we restrict considerations to stacks with more than 60 receiver functions (Fig. 2B), the noise levels in linearly stacked receiver functions are 0.03–1.0% of the amplitude of the P-wave (Fig. 3), much less than the amplitude of linearly stacked P410s and P660s phases (2–6% of the amplitude of the P-wave). Improvement in S/N ratios is achieved with an nth-root ($n = 2$) stacking process [18], a non-linear method that suppresses random noise and enhances coherent signals. The relative amplitudes of nth-root-stacked P410s and P660s phases are 10–80 times greater than the levels of similarly processed and stacked records of noise immediately before the corresponding P arrivals (Fig. 2E,H,K).

Rather than using the peaks of P410s and P660s as in the previous study [13], the arrival times of the converted phases are weighted linearly by the value of the amplitude of the waveform of the converted phases. For symmetric converted-phase waveforms, the expected picks of the new method are the peaks of the waveforms, but these picks are less susceptible to random noise than in the previous study [13]. Bootstrap analysis [19] shows that the greater number of high-quality receiver functions than in the previous study and the new arrival-time picking method yield 95% confidence limits on the arrival times that are much smaller than the lateral variation in the arrival times of the converted phases (Fig. 2G,J).

3. Transition-zone thickness

Images of P410s and P660s arrivals derived by nth-root stacking of receiver functions, and P660s–P410s differential arrival times, are shown along selected profiles in Fig. 2. To the north of Iceland, variations in P410s and P660s times are positively correlated and comparable in magnitude (Fig. 2C), reflecting the dominant influence of velocity heterogeneities shallower than the 410-km discontinuity because of the nearly identical paths of P660s and P410s over that depth interval. P660s–P410s differential times, which provide information on the thickness of the transition zone, are not sensitive to heterogeneities shallower than the 410-km discontinuity and are similar to that predicted by the iasp91 global seismic velocity model [15] (Fig. 2D). The positive correlation between P410s and P660s times breaks down beneath central and southern Iceland (Fig. 2F,I); however, where observed P660s–P410s differential times are less than predicted by iasp91 (23.9 s) by as much as 1.6 s (Figs. 2G,J and 3).

Excluding central and southern Iceland, the average differential time beneath the remaining areas is 24.2 ± 0.1 s, comparable to, and within the uncertainty of, values for the mantle beneath the southern East Pacific Rise (24.7 ± 0.6 s) [20] as well as the global average (24.0 ± 0.6 s) [21]. Observations of long-period SS precursors indicate that the mantle transition zone in most oceanic areas is unlikely to be significantly thicker than in the iasp91 model [12].

The mantle transition-zone thickness beneath central and southern Iceland implied by the P660s–P410s differential times is less than beneath surrounding areas by $\sim$19 km. Given Clapeyron slopes of 2.9 and –2.1 MPa/K for the 410- and 660-km discontinuities [22], respectively, the reduction in the transition-zone thickness is equivalent to an excess temperature of 140 K. The finite sizes of both the Fresnel zone of converted phases and the patches used for stacking [13] tend to smooth lateral variations in discontinuity depths. For example, for a dome-shaped elevation of the 660-km discontinuity having a radius of 150 km and a height of 15 km, we can retrieve from similarly processed and stacked synthetic waveforms about 65% of the maximum amplitude of the topography over a 400-km-diameter region. Furthermore, lower velocities associated with excess temperatures within the transition zone inferred from the transition-zone thickness anomaly would increase the P660s time ($\sim$0.2 s per 100 K excess temperature) and decrease the apparent reduction in the transition-zone thickness. Our estimate of the excess temperature should therefore

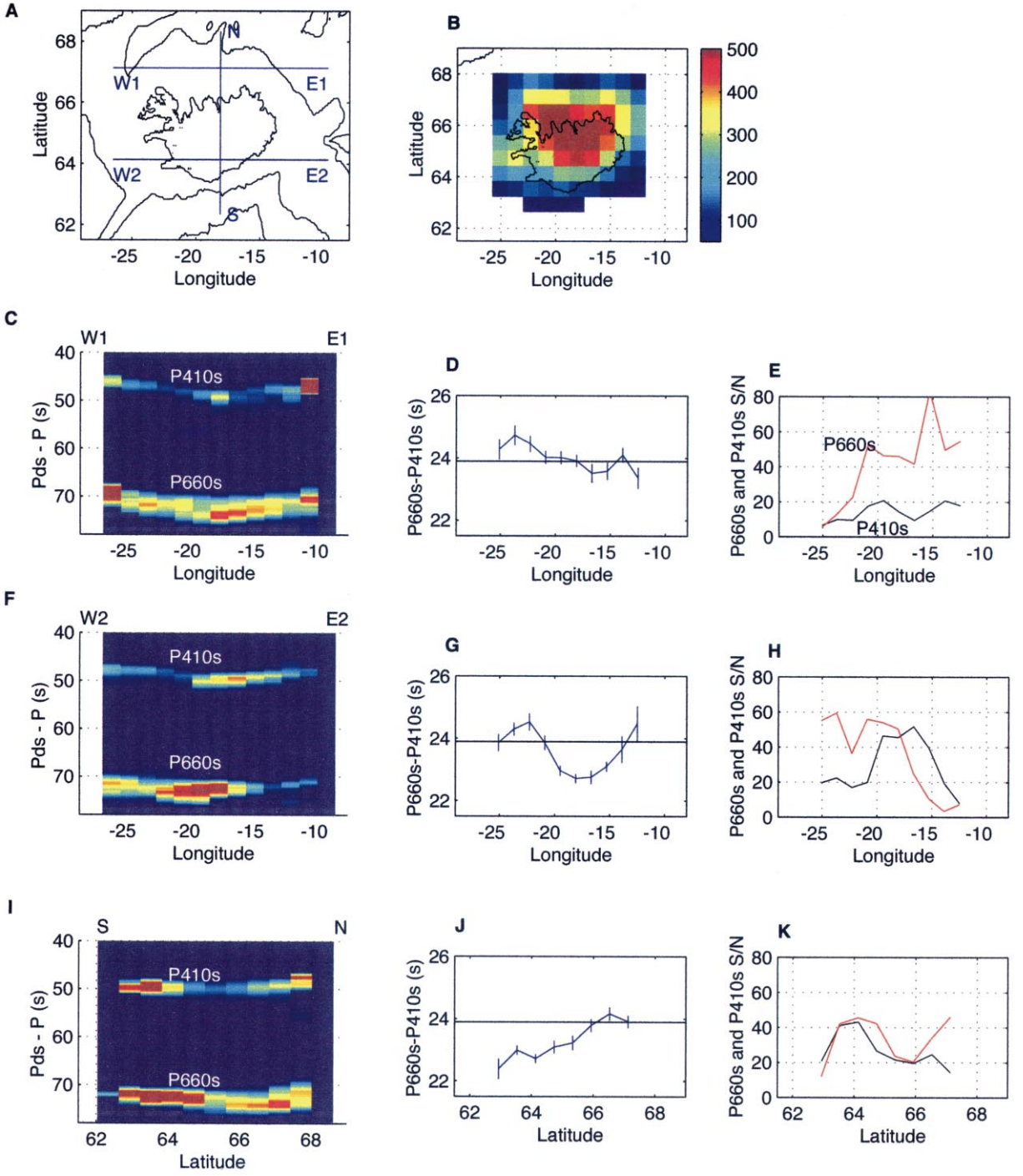

be regarded as only an apparent value and most likely a lower bound. With these factors taken into consideration, an apparent excess temperature of at least 140 K is in agreement with estimates of the thermal anomaly ($\sim$200 K) at the depth of melt generation ($<$200 km) [23], values that reflect averages of the melt-generation and melt-migration processes.

Fig. 2. Images of P410s and P660s in stacked receiver functions and P660s–P410s differential times indicate an anomalously thin transition zone beneath central and southern Iceland. (A) Locations of the profiles of receiver function stacks. (B) The number of receiver functions in each stack at a depth of 660 km. (C) Relative amplitudes of receiver function *n*th-root stacks along an east–west profile north of Iceland. Red and yellow colors represent positive- and relatively higher-amplitude arrivals. Note that the *n*th-root stacking amplifies weak signals in noisy data but does not preserve amplitudes and waveforms. The vertical axis is the time after the compressional-wave (P) arrival. (D) P660s–P410s differential times along this northern profile compared with that predicted (horizontal line) for the iasp91 global model [15]. The differential times and their 2σ errors are estimated using a bootstrap method. A 1-s change in differential time is equivalent to an about 10-km change in transition-zone thickness. (E) The S/N ratio of identified P410s (black line) and P660s (red line) phases along this northern profile, obtained by dividing the amplitude of the converted phases by the levels of similarly processed and stacked records of noise immediately prior to the corresponding P arrivals. (F–H) Relative amplitude, differential times, and S/N ratios ratios of converted phases along an east–west profile through central Iceland. (I–K) Relative amplitude, differential times, and S/N ratios of converted phases along a north–south profile through central Iceland.
←

We note that the southern boundary of the transition-zone anomaly beneath Iceland (Fig. 4) remains to be mapped, and we therefore cannot rule out the possibility that the transition-zone anomaly beneath Iceland is part of a large regional anomaly that extends south of Iceland. However, the close proximity of the transition-zone anomaly to the low-velocity body in the shallow mantle [24–26] and the fact that the thinner transition zone does not follow the geometry of the plate boundary support the interpretation that the transition-zone anomaly beneath Iceland is associated with the Iceland mantle plume.

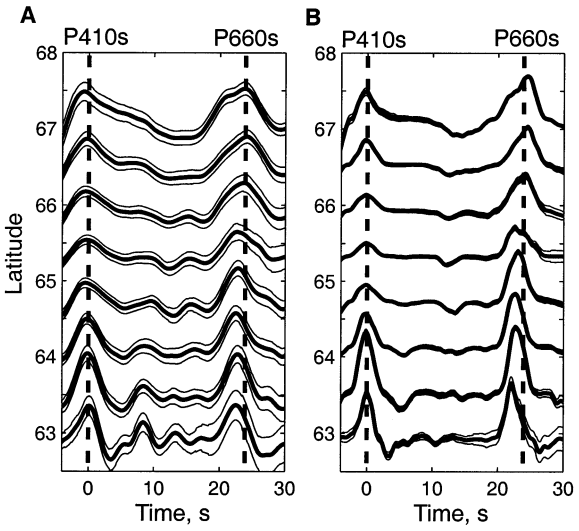

Fig. 3. Waveforms of linearly stacked (A) and *n*th-root-stacked (B) receiver functions along the north–south profile through central Iceland and their 95% confidence limits (thin lines). The traces are aligned on the P410s arrival time determined by bootstrap [19] and weighted linearly by the value of the amplitude of the waveform of the converted phase. They are normalized by a constant for each panel and plotted as a function of latitude in degrees. The vertical lines mark the values predicted for the iasp91 model [15].

4. The 410- and 660-km discontinuities

Within the area of anomalously thin mantle transition zone, the reduction in P660s–P410s differential time correlates with a decrease in P660s arrival time (Figs. 2I and 5) and does not show a comparable correlation with P410s arrival time (Fig. 5). The individual and differential Pds times reported here have not been corrected for velocity heterogeneity or anisotropy in the upper mantle, but such corrections do not change the general relationships between differential times and individual arrival times of the converted phases [13]. Any correction for delays expected from greater-than-normal temperatures in the transition zone inferred from the transition-zone thickness anomaly would further reduce P660s times and strengthen the correlation between differential and P660s times.

Several conditions pertinent to the Iceland plume may reduce the depth to the 410-km discontinuity and thus at least partially balance the effect of excess temperatures and a positive Clapeyron slope for the 410-km discontinuity. Along the Reykjanes Ridge, basalt samples show increasing H_2O concentrations toward Iceland, indicating that Icelandic basalts prior to degassing

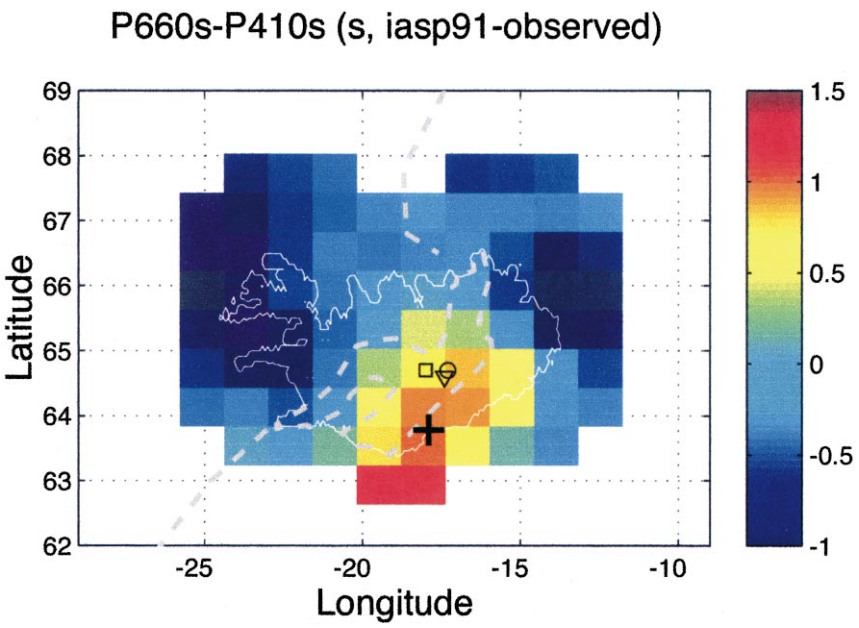

Fig. 4. Map view of differences between the observed P660s–P410s differential times and the value predicted for the iasp91 model [15]. Red and yellow colors indicate significantly smaller differential times (thinner mantle transition zone) than in iasp91, while blue colors denote normal or somewhat greater differential times (normal or slightly thicker mantle transition zone). The cross marks the center of the mapped area of thinned transition zone. The circle, square, and triangle represent the locus of thickest crust and the centers of low S and P velocities in the uppermost mantle [24], respectively. The image has been smoothed by a two-dimensional, five-point moving average. Dashed gray lines delineate Icelandic volcanic zones and the axis of the Mid-Atlantic Ridge.

have at least 0.35 wt% H_2O [27], an amount greater than in normal mid-ocean ridge basalt (MORB, 0.1–0.2 wt%) [28]. Since water is preferentially partitioned into the melt, high H_2O concentrations in Icelandic basalts and a higher-than-normal extent of melting beneath Iceland require high concentrations of H_2O in the plume source. H_2O in the $(Mg, Fe)_2SiO_4$ system stabilizes β-spinel, resulting in a broader and shallower α–β transition [29]. The onset of the α–β transformation for a mantle source with 500 ppm H_2O is calculated to occur about 8 km shallower than for a normal MORB source with 200 ppm H_2O [29]. In the postspinel transition, H_2O shifts the phase boundary (the 660-km discontinuity) to higher pressures than in the anhydrous case [30].

Other possible mechanisms for reducing the depth of the 410-km discontinuity beneath Iceland include a lower-than-normal Al content in the plume source [11] and a non-equilibrium condition at the depth of phase transformation [31]. It has been suggested that the Iceland plume source consists of an Al-poor, refractory matrix and veins and blobs containing enriched components [32]. The geochemical signature of depletion in Icelandic basalts, however, can also be matched by a multicomponent mixing model involving two incompatible, trace-element-enriched components and the usual normal MORB source [33]. A mantle source with a lower-than-normal Al content and a higher-than-normal percentage of olivine would be predicted to display greater-than-normal velocity jumps at the 410- and 660-km discontinuities and high amplitudes for phases converted at the discontinuities. The amplitudes of the linearly stacked P410s and P660s phases we observe, in fact, are correlated with the reduction in P660s–P410s differential time. In particular, the largest P410s amplitude beneath southern Iceland (near 63.5°N, 17.5°W, at 4–5% of the amplitude of the P-wave on the vertical component) is nearly twice as large as beneath surrounding areas. In

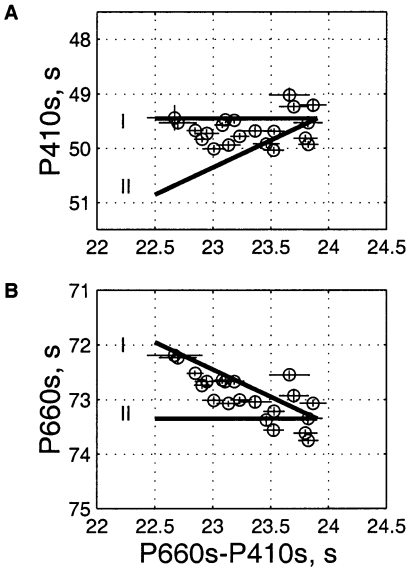

Fig. 5. Correlations between the P660s–P410s differential times and individual arrival times of the P410s (A) and P660s (B) phases in the area of anomalously thin transition zone. The straight lines represent two end-member models in which the reduction in P660s–P410s differential times is caused by (I) a decrease in P660s arrival time (relative to the P arrival time), or (II) an increase in P410s arrival time.

contrast to the situation at 410-km depth, variations in the Al content of the mantle should have little effect on the depth of the transformation between γ-spinel and perovskite plus magnesiowüstite [11].

If the upper-mantle phase transitions within the upwelling plume conduit are limited by nucleation and kinetics [31], then rather than thermodynamic equilibrium the 660-km discontinuity as well as the 410-km discontinuity would be shoaled within the plume. Because the transformation from perovskite plus magnesiowüstite to γ-spinel occurs over a narrow pressure interval [11], any non-equilibrium effect on the depth of the 660-km discontinuity is unlikely to be substantially greater than that on the depth of the 410-km discontinuity and, in any case, is probably much less than ~20 km.

Of the possible contributors to reducing the depth of the 410-km discontinuity within the Iceland plume – high H_2O content, low Al content, or a non-equilibrium phase transition – none are likely to reduce the thickness of the mantle transition zone. The low values of P660s–P410s differential time beneath central and southern Iceland are therefore predominantly the consequence of the excess temperature of the plume and the positive and negative Clapeyron slopes of the phase transformations near 410- and 660-km depth, respectively. This inference is consistent with the results of recent mineral-physics experiments [34,35] that the 660-km discontinuity corresponds to the transformation between γ-spinel and perovskite plus magnesiowüstite, rather than the garnet–perovskite transformation [11,36], which has a positive Clapeyron slope.

5. Tilting of the Iceland plume and implications for mantle flow beneath Iceland

Most of the area of thinner transition zone (defined as the region where P660s–P410s differential times are less than predicted by iasp91 by at least 0.5 s, or the transition-zone thickness is at least 5 km thinner than in iasp91) resolved in our study is south of central Iceland (Fig. 4). The center of the mapped area of thinned transition zone, defined as the average location of the thinner-than-normal transition zone weighted linearly by the magnitude of reduction in transition-zone thickness, is beneath southern Iceland near 63.8 ± 0.1°N, 17.9 ± 0.1°W (Fig. 4). If the smallest P660s–P410s differential time indicates the highest excess temperature at the center of the plume, then the center of the transition-zone anomaly may be south of 63.8°N by 1° of latitude or more (Figs. 2J and 4).

The center of the area of thinned transition zone lies south of the inferred location of the plume at the depth of primary melt generation (< 200 km) by at least 100 km. The location of the plume core in the shallow mantle is constrained in several ways. First, crustal thickness can be regarded as a proxy for integrated melt production in the upper 200 km or so of mantle. Increased temperature and mass flux within the rising plume conduit are expected to result in greater than average melt production and thus

an anomalously thick crust above the plume core. Inversions of waveforms of surface waves from local earthquakes [37], travel times of refracted phases [38], and receiver functions for local crustal structure [39,40] show that the center of the area of the thickest crust (in excess of 40 km) is near 64.7°N, 17.3°W, coinciding with a regional Bouguer gravity minimum [41]. Second, tomographic inversions of body-wave travel-time delays show a low-velocity anomaly in the shallow upper mantle (<250 km) beneath central Iceland near 64.7°N, 17.5°W [24–26]. Third, olivine tholeiite and picrite samples from the Icelandic neovolcanic zones reveal a 'plateau' of high $^3He/^4He$ ($\sim 20\ R/R_a$, sample values normalized by the atmospheric value) that is approximately 100 km in diameter and coincides with the Bouguer gravity minimum, the maximum crustal thickness, and the upper-mantle low-velocity anomaly [42]. Breddam et al. [42] suggest that this zone of elevated $^3He/^4He$ ratios outlines the plume conduit at the depth of melting of the Iceland mantle plume.

The offset between the center of the transition-zone thickness anomaly and the center of shallow measures of plume influence suggests that the plume is tilted in the upper mantle, with an angle of tilt of at least 9° from the vertical (Fig. 6). For comparison, the sharpness of the bend in the Hawaiian–Emperor volcanic chain implies that the deflection of the underlying plume due to a change in plate motion is less than 200 km [43].

Current tomographic models of the Icelandic upper mantle provide no strong evidence either for or against a tilted Iceland mantle plume. Inversions of the ICEMELT data by Wolfe et al. [24] show that the center of the low P-wave velocity at 300-km depth is noticeably south of the center of the velocity anomaly at 125-km depth, but there is no lateral offset of the center of the anomaly for S-wave velocity. Foulger et al. [25] found from inversions of HOTSPOT data that the low-velocity anomaly appears to be elongated north–south at depths of 250–400 km and interpreted this as evidence that the low-velocity anomaly extends no deeper than the mantle transition zone. While Allen et al. [26], who inverted data from the same experiment, found a similar elongation of the low-velocity anomaly for high-frequency P-waves, they report a more circular low-velocity anomaly for low-frequency P- and S-waves. The differences between P- and S-velocity models and the presence or absence of a lateral offset of the center of the low-velocity anomaly in the uppermost 400 km may result from limits to resolution at depths near 400 km beneath Iceland from the limited aperture of the seismic networks (Fig. 1) and the assumption of mantle isotropy. Furthermore, a lower viscosity in the asthenosphere than in the deeper mantle [44] could result in a conduit more vertical in the asthenosphere than at greater depths. In the following discussion, a straight plume conduit is considered as a first-order approximation.

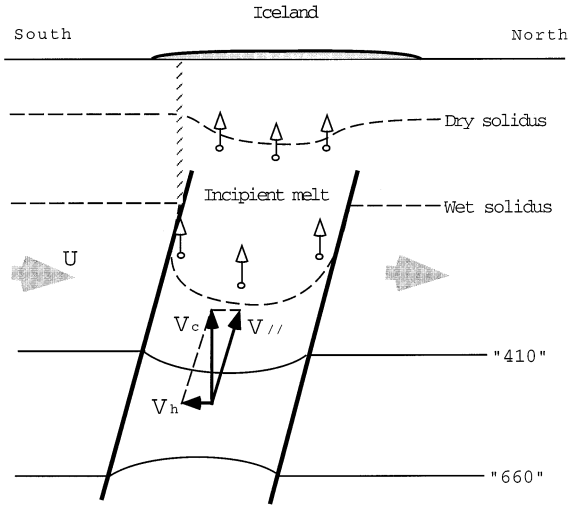

Fig. 6. Schematic north–south cross-section through the center of the Iceland mantle plume. The southward shift of the center of the transition-zone thickness anomaly relative to central Iceland, where the thickest crust, minimum Bouguer gravity, and highest $^3He/^4He$ are found, indicates a tilted plume conduit. Incipient hydrous melts migrate vertically to the surface and erupt as high-$^3He/^4He$ alkaline basalts in the southern portions of the eastern volcanic zone. The rising velocity of the plume conduit (V_c) can be decomposed into a component parallel to the plume conduit ($V_{//}$) and a horizontal component (V_h) at least partly balancing a generally northward flow of the upper mantle beneath the North Atlantic region near Iceland (U).

Tilting of the plume may account for some of the apparent north–south elongation of both the transition-zone thickness anomaly (Fig. 4) and the low-velocity anomaly beneath southern Iceland

[25,26]. The tilt could also have important implications for the distribution of geochemical anomalies in Icelandic basalts. Alkaline basalts from southern Iceland high in $^3He/^4He$ (13.9–26 R/R_a) have been interpreted as products of low-degree, volatile-rich hydrous melting from the plume mantle deflected horizontally below a high-viscosity lid having a base at the dry solidus [42]. Such a mechanism, however, should lead to a symmetric distribution of high-$^3He/^4He$ alkaline basalts about the center of the plume, but high-$^3He/^4He$ alkaline basalts are not observed in the northern volcanic zone [42]. The tilted plume model provides a simple and self-consistent alternative mechanism: Incipient hydrous melts generated within the plume conduit migrate vertically to the surface and erupt as high-$^3He/^4He$ alkaline basalts in southern Iceland (Fig. 6).

A tilt in the Iceland plume indicates relative shear between horizontal flows at asthenospheric levels and those at greater depth. The relative shear can result from southward flow of the upper part of the lower mantle, northward flow of the Icelandic upper mantle, or a combination of the two in a reference frame having no net rotation of the mantle. Recent mantle circulation models, in which driving forces are density heterogeneities constrained by global seismic tomographic models, predict southward flow of the lower mantle beneath Iceland [45]. If the Iceland plume originates at or near the core–mantle boundary, as has been inferred from the detection of an ultralow-velocity zone above the core–mantl boundary beneath Iceland [46], then deformation of the plume conduit by such lower-mantle flow would yield a plume source located near 60–61°N, 19–22°W [45], and a tilted plume conduit with a direction and magnitude of tilt in the upper mantle consistent with our observations.

Splitting of shear waves recorded at ICEMELT seismic stations indicates that the direction of fast polarization of steeply incident shear waves in the Icelandic upper mantle is approximately north–south [47]. This pattern of shear-wave splitting cannot be explained by simple models of horizontally diverging flow driven either by plate spreading or by radial horizontal flow from the center of the hotspot. Given that shear-wave splitting arises primarily in the upper 300 km of the mantle [48], the observed pattern of shear-wave splitting has been interpreted as the result of a combination of plate-induced flow and a generally northward flow of the upper mantle beneath the North Atlantic region near Iceland [47]. This interpretation is consistent with the direction of tilt of the plume. Entrainment of plume material by northward asthenospheric flow beneath Iceland also provides a possible reconciliation of northward extension of the upper-mantle low-velocity anomaly into northern Iceland [25,26] and the normal transition zone beneath this region. Generally northward upper-mantle flow is not only predicted from some simple kinematic models in which flow is determined by the mass flux imposed by plate motion [49] but also from dynamic models that include flows due to internal mantle density heterogeneities inferred from seismic tomography (B. Steinberger, personal communication, 2001). It contradicts, however, an interpretation [50] of the apparently more pronounced geochemical and geophysical anomalies along the Mid-Atlantic Ridge south of Iceland than those to the north as the result of shallow southward mantle flow.

The two kinematic explanations for the tilt of the plume (northward asthenospheric flow and southward flow of the upper part of the lower mantle) are not mutually exclusive, but they predict opposite effects on the surface motion of the Iceland hotspot. Southward flow of the lower mantle predicts a southward component of motion of the surface hotspot, as the tilted conduit rises in the mantle [5,45]. Northward flow of the upper mantle beneath Iceland, in contrast, predicts a northward component of motion of the surface hotspot, but such motion is at least in part balanced by southward motion of the hotspot from the rise of the tilted plume conduit. For a relatively slow-moving lower mantle, the tilt of the plume conduit and hotspot location adjust quickly to quasi steady-state after changes in upper-mantle flow [45]. The north–south directions of fast polarization of shear waves [47] suggest that the rates of north–south asthenospheric flow are greater than the plate velocity (18 km/Ma full spreading rate) so that the net flow direction

and thus the strain-induced, lattice-preferred orientation in the asthenosphere beneath Iceland are approximately north–south. For a plume having a radius of 100 km [24–26], an excess temperature of 200 K [23], a tilt of 10°, and an average viscosity of the upper mantle of 10^{20}–10^{21} Pa s [44], the predicted southward horizontal motion of the hotspot due to the rise of the tilted conduit [5,45] is 5–50 km/Ma. Significant southward asthenospheric flow beneath Iceland can be ruled out, because such a flow together with the effect of the rise of the tilted conduit would result in a southward motion of the surface hotspot at a rate greater than the spreading rate. Such a motion, if coherent over $\sim$20 Ma, would be resolvable but is not observed. To maintain a slow-moving or stationary Iceland hotspot, flow of the Icelandic upper mantle must be northward and comparable to the southward horizontal motion of the hotspot due to the rise of the tilted plume (Fig. 6).

Geodynamic interpretations of the tilt of the plume conduit are clearly model dependent and need to be sharpened by a fuller understanding of the history of hotspots and plate motions. Nevertheless, this study provides strong seismological evidence for a tilted plume conduit in the upper mantle, a consequence of large-scale, horizontal mantle flow beneath the surface hotspot.

Acknowledgements

We thank Bergur H. Bergsson, Bjorn Bjarnason, Birgir Bjarnason, Bryndis Brandsdóttir, Haukur Brynjólfósson, Kristinn Egilsson, Pálmi Erlendsson, Gunnar Gudmundson, Eythór Hannesson, Tryggvi Hardarson, Lárus Helgason, Bogi Ingimundarson, Haraldur Jónsson, Einar Kjartansson, A. Kuehnel, R. Kuehnel, Sturla Ragnarsson, Pálmi Sigurdsson, Ragnar Thrudmarsson, and the staff of the National Electric Company of Iceland (Landsvirkjun) for assistance with ICEMELT and HOTSPOT field operations. We also thank Scott King, Jeroen Ritsema, Bernhard Steinberger, Peter van Keken, and an anonymous reviewer for constructive comments. This research was supported by the National Science Foundation under Grants EAR-9316137, OCE-9402991, EAR-9417918, and OCE-9906902.*[SK]*

References

[1] J.T. Wilson, A possible origin of the Hawaiian islands, Can. J. Phys. 41 (1963) 863–870.
[2] W.J. Morgan, Convection plumes in the lower mantle, Nature 230 (1971) 42–43.
[3] P. Molnar, J. Stock, Relative motions of hotspots in the Pacific, Atlantic and Indian Ocean since late Cretaceous time, Nature 327 (1987) 587–591.
[4] J.A. Tarduno, R.D. Cottrell, Paleomagnetic evidence for motion of the Hawaiian hotspot during formation of the Emperor seamounts, Earth Planet. Sci. Lett. 153 (1997) 171–180.
[5] M.A. Richards, R.W. Griffiths, Deflection of plumes by mantle shear flow: experimental results and a simple theory, Geophys. J. 94 (1988) 367–376.
[6] H. Bijwaard, W. Spakman, Tomographic evidence for a narrow whole mantle plume below Iceland, Earth Planet. Sci. Lett. 166 (1999) 121–126.
[7] D. Zhao, Seismic structure and origin of hotspots and mantle plumes, Earth Planet. Sci. Lett. 192 (2001) 251–265.
[8] G.R. Foulger, D.G. Pearson, Is Iceland underlain by a plume in the lower mantle? Seismology and helium isotopes, Geophys. J. Int. 145 (2001) F1–F5.
[9] J. Ritsema, H.J. van Heijst, J.H. Woodhouse, Complex shear wave velocity structure imaged beneath Africa and Iceland, Science 286 (1999) 1925–1928.
[10] C. Mégnin, B. Romanowicz, The three-dimensional shear velocity structure of the mantle from the inversion of body, surface and higher-mode waveforms, Geophys. J. Int. 143 (2000) 709–728.
[11] D.J. Weidner, Y. Wang, Phase transformations: implications for mantle structure, in: S. Karato, A. Forte, R. Liebermann, G. Masters, L. Stixrude (Eds.), Earth's Deep Interior: Mineral Physics and Tomography From the Atomic to the Global Scale, Am. Geophys. Union, Washington, DC, 2000, pp. 215–235.
[12] P.M. Shearer, Transition zone velocity gradients and the 520-km discontinuity, J. Geophys. Res. 101 (1996) 3053–3066.
[13] Y. Shen, S.C. Solomon, I.Th. Bjarnason, C.J. Wolfe, Seismic evidence for a lower-mantle origin of the Iceland plume, Nature 395 (1998) 62–65.
[14] I.Th. Bjarnason, C.J. Wolfe, S.C. Solomon, G. Gudmundson, Initial results from the ICEMELT experiment: body-wave delay times and shear-wave splitting across Iceland, Geophys. Res. Lett. 23 (1996) 459–462.
[15] B.L.N. Kennett, E.R. Engdahl, Traveltimes for global earthquake location and phase identification, Geophys. J. Int. 105 (1991) 429–465.
[16] R.M. Allen, G. Nolet, W.J. Morgan, K. Vogfjörd, B.H.

Bergsson, P. Erlendsson, G.R. Foulger, S. Jakobsdóttir, B.R. Julian, M. Pritchard, S. Ragnarsson, R. Stefánsson, The thin hot plume beneath Iceland, Geophys. J. Int. 137 (1999) 51–63.

[17] K.G. Dueker, A.F. Sheehan, Mantle discontinuity structure from midpoint stacks of converted P to S waves across the Yellowstone hotspot track, J. Geophys. Res. 102 (1997) 8313–8327.

[18] E.R. Kanasewich, C.D. Hemmings, T. Alpaslan, Nth-root stack nonlinear multichannel filter, Geophysics 38 (1973) 327–338.

[19] B. Efron, G. Gong, A leisurely look at the bootstrap, the jackknife, and cross-validation, Am. Stat. 37 (1983) 36–48.

[20] Y. Shen, A.F. Sheehan, K.G. Dueker, C. de Groot-Hedlin, H. Gilbert, Mantle discontinuity structure beneath the southern East Pacific Rise from P-to-S converted phases, Science 280 (1998) 1232–1235.

[21] S. Chevrot, L. Vinnik, J.-P. Montagner, Global-scale analysis of the mantle Pds phases, J. Geophys. Res. 104 (1999) 20203–20219.

[22] C.R. Bina, G. Helffrich, Phase transition Clapeyron slopes and transition zone seismic discontinuity topography, J. Geophys. Res. 99 (1994) 15853–15860.

[23] R.S. White, J.W. Bown, J.R. Smallwood, The temperature of the Iceland plume and origin of outward-propagating V-shaped ridges, J. Geol. Soc. Lond. 152 (1995) 1039–1045.

[24] C.J. Wolfe, I.Th. Bjarnason, J.C. VanDecar, S.C. Solomon, Seismic structure of the Iceland mantle plume, Nature 385 (1997) 245–247.

[25] G.R. Foulger, M.J. Pritchard, B.R. Julian, J.R. Evans, R.M. Allen, G. Nolet, W.J. Morgan, B.H. Bergsson, P. Erlendsson, S. Jakobsdóttir, S. Ragnarsson, R. Stefánsson, K. Vogfjörd, The seismic anomaly beneath Iceland extends down to the mantle transition zone and no deeper, Geophys. J. Int. 142 (2000) F1–F5.

[25] R.M. Allen, G. Nolet, W.J. Morgan, K. Vogfjörd, B.H. Bergsson, P. Erlendsson, G.R. Foulger, S. Jakobsdóttir, B.R. Julian, M. Pritchard, S. Ragnarsson, R. Stefánsson, Imaging plume-ridge interaction in the mantle beneath Iceland, J. Geophys. Res., in press.

[27] P. Poreda, J.-G. Schilling, H. Craig, Helium and hydrogen isotopes in ocean-ridge basalts north and south of Iceland, Earth Planet. Sci. Lett. 78 (1986) 1–17.

[28] P. Michael, Regionally distinctive sources of depleted MORB: evidence from trace elements and H_2O, Earth Planet. Sci. Lett. 131 (1995) 301–320.

[29] B.J. Wood, The effect of H_2O on the 410-kilometer seismic discontinuity, Science 268 (1995) 74–76.

[30] T. Inoue, Y. Higo, T. Ueda, Y. Tanimoto, T. Futagami, T. Irifune, The effect of H_2O and CO_2 on α-β-γ and postspinel phase transformation of olivine, EOS Trans. Am. Geophys. Union 82 (2001) F1129–F1130.

[31] V.S. Solomatov, D.J. Stevenson, Can sharp seismic discontinuities be caused by non-equilibrium phase transformations?, Earth Planet. Sci. Lett. 125 (1994) 267–279.

[32] A.C. Kerr, A.D. Saunders, J. Tarney, N.H. Berry, V.L. Hards, Depleted mantle-plume geochemical signature no paradox for plume theories, Geology 23 (1995) 843–846.

[33] B.B. Hanan, J. Blichert-Toft, R. Kingsley, J.-G. Schilling, Depleted Iceland mantle plume geochemical signature: artifact of multicomponent mixing? Geochem. Geophys. Geosyst. 1 (2000).

[34] S.-H. Shim, T.S. Duffy, G. Shen, The post-spinel transformation in Mg_2SiO_4 and its relation to the 660-km seismic discontinuity, Nature 411 (2001) 571–574.

[35] L. Chudinovskikh, R. Boehler, High pressure polymorphs of olivine and the 660-km seismic discontinuity, Nature 411 (2001) 574–577.

[36] K. Hirose, Y. Fei, S. Ono, T. Yagi, K. Funakoshi, In situ measurements of the phase transition boundary in $Mg_3Al_2Si_3O_{12}$: implications for the nature of the seismic discontinuities in the Earth's mantle, Earth Planet. Sci. Lett. 184 (2001) 567–573.

[37] R.M. Allen, G. Nolet, W.J. Morgan, K. Vogfjörd, M. Nettles, G. Ekström, B.H. Bergsson, P. Erlendsson, G.R. Foulger, S. Jakobsdóttir, B.R. Julian, M. Pritchard, S. Ragnarsson, R. Stefánsson, Plume driven plumbing and crustal formation in Iceland, J. Geophys. Res., in press.

[38] F.A. Darbyshire, I.Th. Bjarnason, R.S. White, Ó.G. Flóvenz, Crustal structure above the Iceland mantle plume imaged by the ICEMELT refraction profile, Geophys. J. Int. 135 (1998) 1131–1149.

[39] F.A. Darbyshire, K.F. Priestley, R.S. White, R. Stefánsson, G.B. Gudmundsson, S.S. Jakobsdóttir, Crustal structure of central Iceland from analysis of teleseismic receiver functions, Geophys. J. Int. 143 (2000) 163–184.

[40] Z. Du, G.R. Foulger, Variation in the crustal structure across central Iceland, Geophys. J. Int. 145 (2001) 246–264.

[41] G. Thorbergsson, I.Th. Magnússon, G. Pálmason, Gravity data and a gravity map of Iceland, Report OS-93027/JHD-07, Orkustofnun Íslands, 1993.

[42] K. Breddam, M.D. Kurz, M. Storey, Mapping out the conduit of the Iceland mantle plume with helium isotopes, Earth Planet. Sci. Lett. 176 (2000) 45–55.

[43] R.W. Griffiths, M.A. Richards, The adjustment of mantle plumes to changes in plate motion, Geophys. Res. Lett. 16 (1989) 437–440.

[44] K. Lambeck, P. Johnston, The viscosity of the mantle: evidence from analyses of glacial-rebound phenomena, in: I. Jackson (Ed.), The Earth's Mantle: Composition, Structure, and Evolution, Cambridge University Press, New York, 1998, pp. 461–502.

[45] B. Steinberger, Plumes in a convecting mantle: models and observations for individual hotspots, J. Geophys. Res. 105 (2000) 11127–11152.

[46] D.V. Helmberger, L. Wen, X. Ding, Seismic evidence that the source of the Iceland hotspot lies at the core–mantle boundary, Nature 396 (1998) 251–255.

[47] I.Th. Bjarnason, P.G. Silver, G. Rümpker, S.C. Solomon,

Shear wave splitting across the Iceland hotspot: results from the ICEMELT experiment, J. Geophys. Res., in press.
[48] S. Karato, P. Wu, Rheology of the upper mantle A synthesis, Science 260 (1993) 771–778.
[49] B.H. Hager, R.J. O'Connell, Kinematic models of large-scale flow in the Earth's mantle, J. Geophys. Res. 84 (1979) 1031–1048.
[50] C.G. Chase, Asthenospheric counterflow: a kinematic model, Geophys. J. R. Astron. Soc. 56 (1979) 1–18.